IEEE Access
Multidisciplinary | Rapid Review | Open Access Journal

Received May 7, 2018, accepted June 3, 2018, date of publication June 6, 2018, date of current version July 12, 2018.

Digital Object Identifier 10.1109/ACCESS.2018.2844402

A Novel Signal Acquisition System for Wearable Respiratory Monitoring

GUO DAN[1,2], JUNHAO ZHAO[1], ZIHAO CHEN[1,2], HUANYU YANG[1], AND ZHEMIN ZHU[2]

[1]School of Biomedical Engineering, Health Science Center, Shenzhen University, Shenzhen 518060, China
[2]Shenzhen Institute of Neuroscience, Shenzhen 518057, China

Corresponding author: Guo Dan (danguo@szu.edu.cn)

This work was supported in part by the Shenzhen Science and Technology Innovation Council under Grant JCYJ20170818141853626 and in part by the Shenzhen Science and Technology Innovation Council under Grant JCYJ20160608173106220.

ABSTRACT In this paper, a novel human respiration detection method based on angular velocity is proposed for continuous acquisition and analysis of respiratory signals. Using patient-specific information derived from a wearable sensor, our proposed system is capable of monitoring human respiration and assists in identifying potential respiratory disorders by relying on pre-defined simple procedures. Specifically, our signal verification platform is equipped with a carbon dioxide concentration detection device in order to acquire a synchronous signal. In addition, a median filter method is used to extract the respiratory waveform from the original signal. The obtained angular velocity waveform pertaining to human respiration is then compared to the respiratory carbon dioxide concentration waveform, and the validity of our designated parameters is verified. The test results demonstrate that our implemented system is appropriate for unobtrusive respiratory signals acquisition and analysis; therefore, it can be considered a potential alternative for physiological monitoring and respiratory disorders screening.

INDEX TERMS Physiological monitoring, wearable sensors, median filter, angular velocity, respiratory phase.

I. INTRODUCTION

Due to significant advances in technology, there is a vital need for economical and longer healthcare at any time. In addition, the emerging innovative technologies have totally changed the landscape of the traditional health monitoring techniques, such as examining the patient's health status through physiological parameters [1], [2]. Breathing (or respiration) is the biological process of gas exchange between an organism (human body) and the surrounding environment. It is well-known that an orderly execution of gas exchange is vital to the normal metabolism of every human being. The measurement of human respiration is crucial to the diagnosis and monitoring of a wide range of respiratory, pulmonary and cardiovascular disorders. For instance, Chronic Obstructive Pulmonary Disease (COPD) [3], [4], which can be considered as the fourth leading cause of death worldwide by 2030 due to an increase in smoking rates and demographic changes in many countries [5]. There had been extensive studies that have made significant breakthroughs in the direction in which sensors are used to monitor vital signs signals [6]. Moreover, with the help of big data analysis, long-term monitoring can help to examine potential respiratory diseases [7]. Initial diagnosis of insidious respiratory diseases can ensure quick treatment using first-aid to reduce the risks, which may be expected in the coming stages of human life [8].

Several techniques have already been proposed and suggested for respiration monitoring. For example, Bradley et al. designed a carbon dioxide detection device to study transient and steady-states effects on respiratory frequency and depth mechanism [9]. However, their research has some limitations, e.g., most of the time the cannula significantly hampers both the convenience and comfort of the patients. A respiratory plethysmography was used by Leino *et al.* [10]. Moreover, due to poor and static stability mechanism, this method is inappropriate and displays clear and large deviations in signals during long-term monitoring. Lee and Cho [11] proposed a bio-impedance (BI) sensor that is located at the abdomen to detect volume change during inhalation and exhalation for respiration monitoring. However, bio-impedance is an electrical impedance that depends on the various composites of the body, and is uncomfortable to users [12]. Fung *et al.* [13] employed Radar technology to detect the movement of diaphragm. Yoon *et al.* [14]

developed tri-axial accelerometer and gyroscope based techniques for analyzing respiratory waveforms. By placing the sensor in the thoracic region of the participants, Yoon investigated real-time monitoring of the respiratory signals and checked its feasibility in medical applications. In addition, they have found that the thoracic region is not the best choice to deploy the sensors. Previous researchers have explored that suprasternal notch provides more robust results with less gender variability than most of the methods [15]. In this system, the angular velocity based respiratory monitoring system is proposed to detect the parameter of respiratory information. This presents the potential system for ease and comfort by adopting angular velocity for respiration measurement. This paper adopts and validates the respiratory signals derived from suprasternal angular velocity in both male and female subjects. The respiratory detection used in this research provides a novel and effective method and can be easily combined with other technologies to build a complete and structured life information detection system in the future.

II. METHOD

A. RESPIRATION DETECTION MECHANISM

Respiration is the biological process of exchanging gases between organisms (e.g., humans) and the surrounding environment. Expansion and contraction of the thoracic cavity causes the lung to inflate (breathing in) and deflate (breathing out) [16]. The sternum, or breastbone, is located in the center of the chest then raised and pushed out by the built-in respiratory muscles during inhalation. The suprasternal notch is located at the superior border of the sternum, while inertial sensor is positioned in such a way that its upper side touches the skin of trachea and lower side must be interconnected with the skin of the suprasternal notch. During respiration, the sensor area registers a relative fluctuation in between higher and lower levels [17]. The chosen location is insensitive to both male and female genders, and can be used to accurately detect respiratory signals.

Euler's angle formula is the best way to determine the exact position of the fixed-point rotation from the groups of parameters, namely, the Pitch angle, the Roll angle and the Yaw angle [18], which can help in finding the object's movement, as depicted in Fig 1 (a) around X, Y and Z-axis with respect to the original coordinate system accordingly. In this system, the Roll angle was used to obtain the respiratory waveform, while Euler's angle is the integral of the angular velocity, which is the favorite choice for high accuracy, low noise level, and better amplitudes over acceleration. Therefore, this study adopts angular velocity for human respiration measurement. The inertial sensors are attached to the suprasternal notch and rotates with each breathing movement, resulting in angular velocity and output signal changing [19]. As shown in Fig. 1 (b), the ZOY surface of the sensors is attached to the skin; and the sensor rotates around the Y axis during respiration. During inhalation, the X-axis

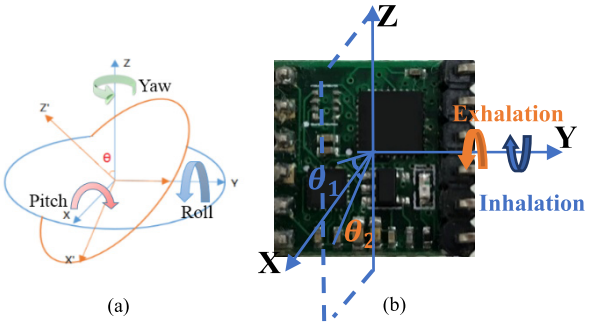

FIGURE 1. (a) Euler angles definition. (b) Inertial sensor motion diagram.

rotates upwards by following the Y axis, then an angle of θ_1 will be formed along with the original X-axis at rest.

The direction of angular velocity during inhalation is positive Y-axis. During exhalation, the X-axis rotates downwards in the direction of the Y-axis and forming θ_2 angle with respect to the original X-axis yat rest. The direction of angular velocity during exhalation is now Y-axis negative. Since the direction of angular velocity differentiates between normal inhalation and exhalation, it can distinguish the inhalation phase from the exhalation one. The baseline respiration can be set-out with the help of angular velocity by examining the resting state of the breathing during sleeping. With continuous breathing, the respiratory signals fluctuate around the baseline.

B. EXPERIMENTAL SETUP

Two test-beds were set-out in this study. First is an inertial sensor platform and second is a carbon dioxide (CO_2) concentration setup. The CO_2 concentration can be considered as the gold standard reference to test the accuracy of the inertial sensor platform for synchronizing the acquisition of both former and later platforms. The CO_2 concentration platform uses a RESPLIVE/TiniStream module from Witleaf Co. Ltd., which helps to open the path for signal acquisition with serial port for data transferring to the connected PC at sampling frequency of 25 Hz, while the inertial sensor platform uses a small, low-cost, and power-efficient INVENSENSOR MPU6050 to detect respiratory signals with sampling frequency of 50 Hz. Moreover, the system can read the data directly and does not require data fusion step, for substantially getting faster data processing rate. Fig. 2 shows the inertial sensor and the CO_2 concentration platforms for our experimental setups.

For data acquisition, the inertial sensor was mounted in the suprasternal notch of the patients using double-sided polyurethane foam tape, and its security was further enhanced by deploying 2 strips over the top of the paper-sheet tape. A nasal cannula was placed directly below the nasal cavity to create the airflow in the respiratory pathway. The collected data were transmitted to the PC and synchronized by compatible software, and then synchronized data were used for subsequent processing.

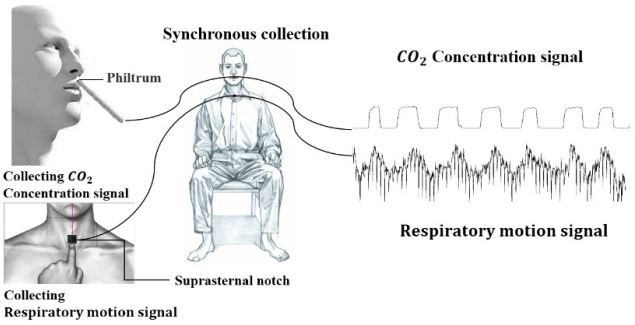

FIGURE 2. Synchronous acquisition system to extract respiratory data.

C. WAVEFORM MEANING AND INTRODUCRTION

The mean difference of the respiratory angular velocity depends on the sensor's location selection. The inertial sensor attached to the suprasternal notch rotates around a Y-axis, which is in parallel to the superior-inferior axis of the human anatomical position. During inhalation, the chest cavity expands until the inhalation ends, and the corresponding angular velocity gradually varies with positive and negative margins. During exhalation, the angular velocity again continuously varies with the same amount but in opposite direction. The turning points for inhalation and exhalation correspond to the regions where the breathing waveform intersects the baseline when no respiration is detected or allowed. For further details, refer to the waveform of the respiratory angular velocity in Fig. 3. The area above the baseline represents the inhalation phase, and the area below represents the exhalation phase. As indicated in the Fig. 3, the waveform fluctuates around the baseline with each breathing movement.

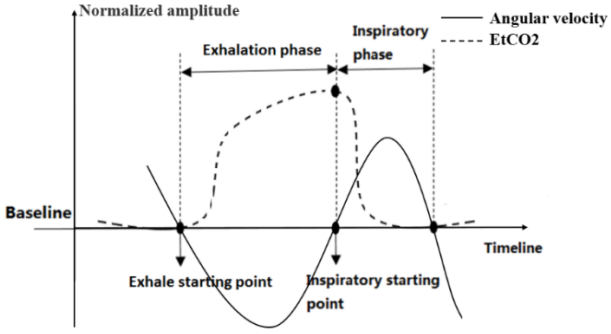

FIGURE 3. Respiratory angular velocity signal and carbon dioxide concentration signal.

Now, the waveform of the respiratory CO_2concentration at the end of the breathing movement is also shown in Figure 3. The waveform consists of four phases: the first phase is the inspiratory baseline, the second is the expiratory ascending branch, the third phase is the alveolar plateau, and the forth phase is the inspiratory descending branch. During exhalation, the mixed gas of the alveoli and the dead space (i.e. the gas of the alveoli and the respiratory tract above the alveoli) are first breathed out at the same time; afterwards, during the plateau, only alveolar gas is exhaled. During inhalation, the CO_2 concentration curve decreases to the baseline rapidly and steeply, and fresh gas then enters the respiratory tract. The starting point of the ascending branch is the beginning of exhalation, and the starting main point of the inspiratory descending branch is the starting point of the inhalation. The frequency and phase of the reference breathing waveform can be determined from the expiratory and inspiratory starting point-based information for comparison and verification.

D. DATA ACQUISITION

To verify the accuracy of respiratory angular rate signals, the respiration of 10 healthy subjects are considered and collected simultaneously; these subjects included 5 males and 5 females, with ages between 21.75 and 28.25 years, with heights between 162.38 cm and 173.62 cm, and weights between 49.88 kg and 80.12 kg, respectively. All subjects understood and agreed to the experimental contents and provided their written consent before the experiment. The experiment used a single channel angular velocity signal acquisition module to collect the respiratory signal placed on the suprasternal notch of the subjects as the sample signal. The use of wired devices ensures the stability of signal transmission.

The speed of respiration varies from subject to subject. Studies have shown that the respiratory phases of different frequencies reveal distinct the accuracy levels. Three unique frequencies such as, a normal frequency, a high frequency and a low frequency are chosen for respiratory signals during the experimental setup. Through our performance analysis, we controlled the breathing frequency by asking the subjects to breathe at the normal frequency 0.25 Hz, the low frequency 0.15 Hz, and the high frequency 0.4 Hz, and the pace is set by a metronome.

In the experiment, the subjects were asked to breathe 10 times and then hold it for 10 seconds, and this is performed based on 3 repetitions of this process. To reduce the interference resulting from changing between breathing at different frequencies, each participant was provided with a 2-minute break before switching the frequency in order to ensure reliability.

III. ALGORITHMS

The acquired data needed to be pre-processed and initially the extracted parameters must be considered for the evaluation. The noise and phase differences were eliminated by preprocessing, which can help identify the inspiratory and expiratory points of the target and the reference signals for further evaluation. Fig. 4 shows the block diagram for respiratory signal processing.

A. PREPROCESSING

The pre-treatment first resamples the two signals to obtain a frequency of 25 Hz. The special position of the sensor causes noises in the signal. This includes the spike noises caused by heartbeat, and in addition to the random noises of the system. The median filter replaces the data in the fixed

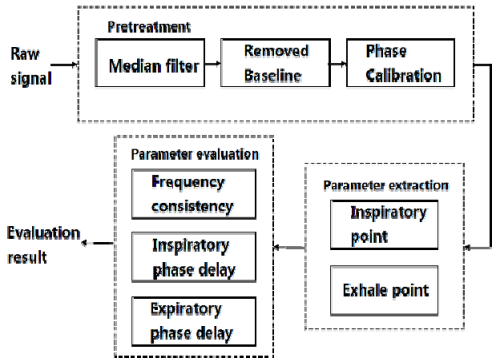

FIGURE 4. Block diagram for processing respiratory signals.

window by filtering the pulse and spike noises in an efficient manner. This method is simple and conductive to hardware implementation, and after testing the chosen median filter window size is 20 [20].

After filtering, the baseline identification process can be used to discriminate between inspiratory and expiratory phases. The median of a fixed length signal during the breathing holding condition was selected as the baseline level. The intersection of the respiratory angular velocity signal obtained by subtracting the baseline value from the de-noised signal and the coordinate axis were considered the starting point of inspiration and expiration [21].

The reference breathing signal has an overall delay relative to the respiratory angular velocity signal. Because the instrument for measuring the CO_2 concentration is pass-through way, it is necessary to gather the breath gas into a small chamber for analysis and processing. And due to the delay of the entire system, the phase shifting is removed. For this purpose, respiratory waveform of the signal is considered and processed after the first time of labored breathing to examine the average delay for the calibration of the whole respiratory time. The phase calibration was based on the initial step of the expiratory level. According to the data test results, the mean value of the system delay was 41 data points, and the variance was 4 data points, between 1.48 and 1.8 seconds.

B. CALCULATION OF RESPIRATORY PARAMETERS

The intersection of the respiratory angular velocity waveform and the transverse axis was identified by the method of intersection point detection to obtain the initial information regarding the starting point of inspiration and expiration [22]. According to the definition of the waveform, the intersection of the signal ascending branch and the horizontal axis is the starting point of the inspiration, and the co-incident waveform descending branch and the horizontal axis is the starting point of the expiration. The inspiration point is identified by finding the data point where the previous data point is less than or equal to zero and the subsequent data section is greater than zero. The expiration is identified by exploring the data parts where the previous data is greater than or equal to zero and the subsequent data series is less than or equal to zero. For the reference breathing waveform, the inspiration and expiration and its starting points are determined by manual identification. According to the waveform meaning, the starting point of the expiratory ascending branch is the beginning of expiration, and the starting point of the inspiratory descending branch is the beginning of inspiration. Fig. 5 reveals the flow chart for identifying phase points, among which T_IN and T_EX are used to store the inspiratory and expiratory starting times, respectively.

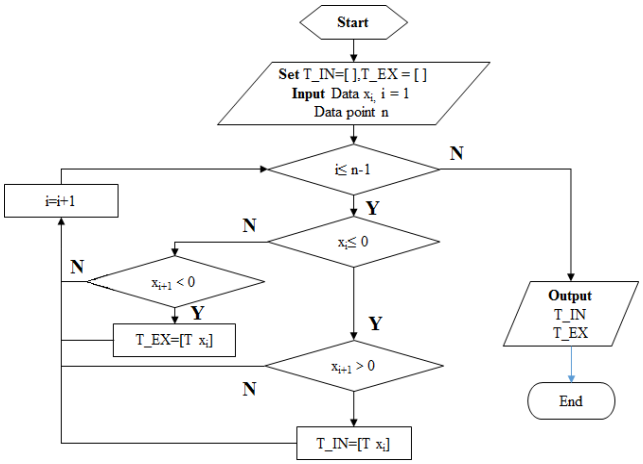

FIGURE 5. Flow chart for identifying phase points.

Here, we present the pseudocode in order to illustrate the flow chart for identifying phase point:

Algorithm identify phase point is

Algorithm 1 Identify phase point Algorithm

Input: Angular rate date x_i with time point T_i,
Date point n
Output: Inspiratory start times T_IN[ ],
Expiratory star times T_EX[ ]
For i=1 to n−1
If $x_i \leq 0$
if $x_{i+1} > 0$ T_IN[ ]=T_i
Else
if $x_{i+1} > 0$ T_EX[ ]=T_i
End If
Next i

In the system, the respiratory verification parameters are the respiratory rate, inspiratory phase delay and expiratory phase delay. The parameters [23] is shown by Eq (1), (2), (3):

$$RR = \frac{1}{\left\{\sum_{i=1}^{N-1} \frac{\left|T_{IN_{i+1}} - T_{IN_i}\right|}{(n-1)}\right\}} \tag{1}$$

$$\Delta T_{in} = \sum_{i=1}^{n-1} \frac{\left(T_{Acc_{IN_{i+1}}} - T_{EtCO2_{IN\,i}}\right)}{(n-1)} \tag{2}$$

$$\Delta T_{ex} = \sum_{i=1}^{n-1} \frac{\left(T_{Acc_{EX_{i+1}}} - T_{EtCO2_{EX\,i}}\right)}{(n-1)} \tag{3}$$

In Eq (1), (2) and (3), RR is the respiratory frequency. ΔT_{in} is the inspiratory phase delay. ΔT_{ex} is the expiratory phase delay. T_{In} is the inspiratory time. Acc_{RR} is the mean value of the respiratory angular velocity frequency. $EtCO_{2RR}$ is the respiratory frequency mean of the respiratory CO_2 concentration waveform. $T_{Acc_{IN}}$ is the inspiratory initial point of the angular velocity. $T_{EtCO_{2IN}}$ is the inspiratory initial point of the respiratory CO_2 concentration waveform. $T_{Acc_{EX}}$ is the expiratory starting point of the angular velocity. $T_{EtCO_{2EX}}$ is the expiratory step of respiratory CO2 concentration waveform.

IV. RESULTS AND DISCUSSION

The consistency between the respiratory angular velocity and the respiratory frequency obtained from reference signal can be represented by the Bland-Altman diagram [24]. Relevant studies have shown that the respiratory frequency obtained from the respiratory angular velocity is able to replace the respiratory frequency obtained from the reference signal. Fig. 6 is the Bland-Altman diagram of two types of signals, corresponding to the consistency evaluation charts of normal frequency breathing, high frequency breathing and low frequency breathing and mixed breathing.

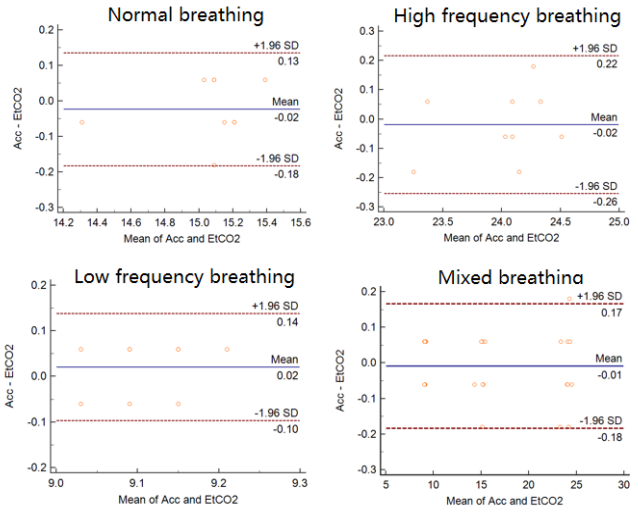

FIGURE 6. Assessment chart for different respiratory rates.

In the chart, the abscissa represents the mean value of the respiratory frequency measured by two methods, and the vertical axis represents the difference between the two methods of measuring the respiratory frequency. In addition, the diagram represents the respiratory angular velocity and the reference respiratory frequency, which lies in the confidence interval at four different types of breathing rates. Regarding dispersion, the high frequency respiration of the two signals is more dispersed. The mixed processing results of the three frequencies indicate that there is a high frequency data point outside of the confidence interval. In general, for normal frequency, high frequency, and low frequency breathings, the respiratory rate obtained by the breathing angular velocity can fulfill the desired requirements, and the respiratory rate can be determined using the angular velocity acquisition device.

The delay in the respiratory angular velocity signal according to the reference signal at the initial step of inspiration and expiration is adopted to evaluate the respiratory phase, and the data can be analyzed by a boxplot of the delay values. The boxplot provides key information about the location and dispersion of the data. As depicted by Fig. 7, this boxplot compares the statistical information pertaining to the inspiratory and expiratory phase delays of four different respiratory frequencies. The chart analyses that delay exist in both the inspiratory and expiratory starting points.

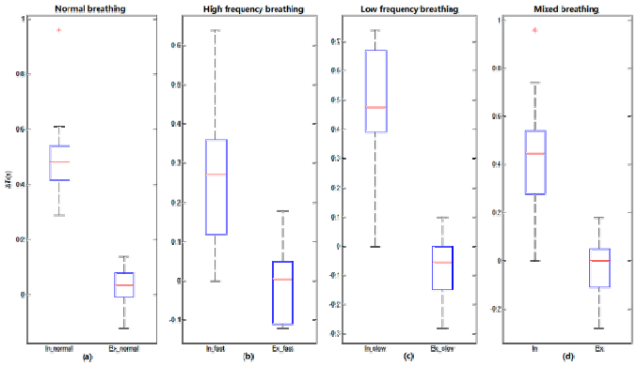

FIGURE 7. Assessment chart for the respiratory phase based on different breathing frequencies.

For the four types of breathing frequencies, the delay in the inspiratory phase step is generally less than that of the starting point of the expiratory phase. This finding occurs because the expiratory starting point is the reference point for calibrating the signal, and the delay time will be entirely focused on the inspiratory starting point. As indicated by the middle position of the boxplot, the average value of the expiratory delay is almost zero, and that average value of the inspiratory delay is generally less than 0.5 seconds. Regarding dispersion, the range for the inspiratory and expiratory starting point delay of the high frequency signals and low frequency signals are larger than that of the normal frequency, indicating that stable information pertaining to normal respiratory signals can be obtained from our respiratory angular velocity signal acquisition device. In general, the delay in the respiratory phase is within an acceptable range.

V. CONCLUSION

Our present results have demonstrated that suprasternal acceleration can provide an accurate measurement of human respiration. The obtained angular velocity can be used to extract the respiratory waveform, calculate the respiratory rate, and retrieve accurate respiratory phase information. Compared with the traditional use of the nasal cannula for obtaining the respiratory signal of the patient, wearing the tiny inertial sensor on the sternum of the patient in this design enables more user comfort. In addition, the data of

CO_2 concentration platform and inertial sensor platform are analyzed by Bland-Altman diagram. The CO_2 concentration is considered as the gold standard for detecting respiratory signals, and is used to verify the feasibility of using the angular velocity signal for respiratory feature extraction. Therefore, our proposed method is deemed suitable for long-term respiration monitoring, and may potentially be used as a gold standard in this field of research.

ACKNOWLEDGMENT

(Guo Dan and Junhao Zhao contributed equally to this work.)

CONFLICT OF INTEREST

The authors declare no conflict of interest.

ETHICS STATEMENT

In this study, all the participants included in the acquisition of respiratory signals provided written informed consent according to specific procedures approved by the IRB of Shenzhen University and Health Science Center Research Ethics Committee. Therefore, all the participants have given written informed consent in accordance with the Declaration of Helsinki.

REFERENCES

[1] M. A. F. Pimentel, P. H. Charlton, and D. A. Clifton, "Probabilistic estimation of respiratory rate from wearable sensors," in *Proc. Wearable Electron. Sensors*. New York, NY, USA: Springer 2015, pp. 241–262.
[2] K. Kim, J. Hong, and C. Kim, "An alarm and response tracking system for the patient-centric perspective," *J. Med. Imag. Health Inform.*, vol. 8, no. 2, pp. 190–195, 2018.
[3] B. McCarthy, D. Casey, D. Devane, K. Murphy, E. Murphy, and Y. Lacasse, "Pulmonary rehabilitation for chronic obstructive pulmonary disease," *Cochrane Database Syst. Rev.*, no. 2, 2015.
[4] Y.-C. Chen, T.-C. Hsiao, and J.-L. Chen, "Better thoracoabdominal synchrony in abdominal breathing: Evidence from complementary ensemble empirical mode decomposition-based Lissajous figure analysis," *J. Med. Imag. Health Inform.*, vol. 5, no. 2, pp. 400–405, 2015.
[5] C. D. Mathers and D. Loncar, "Projections of global mortality and burden of disease from 2002 to 2030," *PLoS Med.*, vol. 3, no. 11, p. e442, 2006.
[6] W. Wu, H. Zhang, S. Pirbhulal, S. C. Mukhopadhyay, and Y. T. Zhang, "Assessment of biofeedback training for emotion management through wearable textile physiological monitoring system," *IEEE Sensors J.*, vol. 15, no. 12, pp. 7087–7095, Dec. 2015.
[7] M. Dion, P. AbdelMalik, and A. Mawudeku, "Big data and the global public health intelligence network (GPHIN)," *Canada Communicable Disease Rep.*, vol. 41, no. 9, pp. 209–214, 2015.
[8] M. J. Tadi, T. Koivisto, and A. Paasio, "Accelerometer-based method for extracting respiratory and cardiac gating information for dual gating during nuclear medicine imaging," *Int. J. Biomed. Imag.*, vol. 2014, no. 5, p. 6, 2014.
[9] G. W. Bradley, C. von Euler, I. Marttila, and B. Roos, "Transient and steady state effects of Co_2 on mechanisms determining rate and depth of breathing," *Acta Physiol.*, vol. 92, no. 3, pp. 341–350, 1974.
[10] K. Leino, S. Nunes, P. Valta, and J. Takala, "Validation of a new respiratory inductive plethysmograph," *Acta Anaesthesiol. Scand.*, vol. 45, no. 1, pp. 104–111, 2001.
[11] W. Lee and S. Cho, "Integrated all electrical pulse wave velocity and respiration sensors using bio-impedance," *IEEE J. Solid-State Circuits*, vol. 50, no. 3, pp. 776–785, Mar. 2015.
[12] S. S. Mirza and M. Z. U. Rahman, "Efficient adaptive filtering techniques for thoracic electrical bio-impedance analysis in health care systems," *J. Med. Imag. Health Inform.*, vol. 7, no. 6, pp. 1126–1138, 2017.
[13] A. Fung, C. Li, and C. Torres, "TH-AB-202-07: Radar tracking of respiratory motion in real time," *Med. Phys.*, vol. 43, p. 3858, Jun. 2016.
[14] J.-W. Yoon, Y.-S. Noh, Y.-S. Kwon, W.-K. Kim, and H.-R. Yoon, "Improvement of dynamic respiration monitoring through sensor fusion of accelerometer and gyro-sensor," *J. Electr. Eng. Technol.*, vol. 9, no. 1, pp. 334–343, 2014.
[15] D. B. Rendon, J. L. R. Ojeda, L. F. C. Foix, D. S. Morillo, and M. A. Fernandez, "Mapping the human body for vibrations using an accelerometer," in *Proc. 29th Annu. Int. Conf. IEEE Eng. Med. Biol. Soc. (EMBS)*, Aug. 2007, pp. 1671–1674.
[16] J. B. West, *Respiratory Physiology: The Essentials*. Philadelphia, PA, USA: Lippincott Williams & Wilkins, 2012.
[17] P. Dehkordi, K. Tavakolian, M. Marzencki, M. Kaminska, and B. Kaminska, "Assessment of respiratory flow and efforts using upper-body acceleration," *Med. Biol. Eng. Comput.*, vol. 52, no. 8, pp. 653–661, 2014.
[18] L. Derafa, A. Benallegue, and L. Fridman, "Super twisting control algorithm for the attitude tracking of a four rotors UAV," *J. Franklin Inst.*, vol. 349, no. 2, pp. 685–699, 2012.
[19] A. Bates, M. J. Ling, J. Mann, and D. K. Arvind, "Respiratory rate and flow waveform estimation from tri-axial accelerometer data," in *Proc. Int. Conf. Body Sensor Netw. (BSN)*, Jun. 2010, pp. 144–150.
[20] K. Kotani, I. Y. Y. Hidaka, and S. Ozono, "Analysis of respiratory sinus arrhythmia with respect to respiratory phase," *Methods Arch.*, vol. 39, no. 2, pp. 153–156, 2000.
[21] C. O'Brien and C. Heneghan, "A comparison of algorithms for estimation of a respiratory signal from the surface electrocardiogram," *Comput. Biol. Med.*, vol. 37, no. 3, pp. 305–314, 2007.
[22] C. Bruser, K. Stadlthanner, S. de Waele, and S. Leonhardt, "Adaptive beat-to-beat heart rate estimation in ballistocardiograms," *IEEE Trans. Inf. Technol. Biomed.*, vol. 15, no. 5, pp. 778–786, Sep. 2011.
[23] D. H. Phan, S. Bonnet, R. Guillemaud, E. Castelli, and N. Y. P. Thi, "Estimation of respiratory waveform and heart rate using an accelerometer," in *Proc. 30th Annu. Int. Conf. IEEE Eng. Med. Biol. Soc.*, Aug. 2008, pp. 4916–4919.
[24] V. Jeyhani, T. Vuorinen, M. Mäntysalo, and A. Vehkaoja, "Comparison of simple algorithms for estimating respiration rate from electrical impedance pneumography signals in wearable devices," *Health Technol.*, vol. 7, no. 1, pp. 21–31, 2017.

GUO DAN received the Ph.D. degree in electrical engineering from the Dalian University of Technology, Dalian, China, in 2003. He is a Professor and the Associate Dean of the School of Biomedical Engineering, Shenzhen University, Shenzhen, China. He is also the Principal Investigator of Shenzhen Institute of Neuroscience, Shenzhen, and the Secretary General of the Shenzhen Society of Biomedical Engineering, Shenzhen. His research mainly focuses on medical equipment and rehabilitation Engineering. He has published several SCI journal articles in the field of his research. He holds over 20 patents. He is serving as the Committee Member of the China Association of Rehabilitation Technology Transformation & Promotion. He is the evaluation committee member of various science foundations and commissions.

JUNHAO ZHAO was born in Zhejiang, China. He received the B.S. degree in biomedical engineering from Wenzhou Medical University in 2016. He is currently pursuing the M.S. degree in biomedical engineering with the Health Science Center, Shenzhen University, Shenzhen, China. His research interests include embedded system design, robot trajectory algorithm, and rehabilitation medicine engineering.

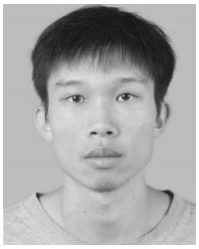

ZIHAO CHEN received the M.Phil. degree in biomedical engineering from the School of Medicine, Shenzhen University, China, in 2015. His research interests include the medical imaging system, application of depth information sensing, and embedded system.

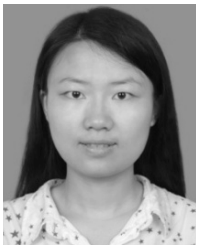

HUANYU YANG received the B.S. degree from Northeastern University, Qinhuangdao, China, in 2014, and the M.S. degree in biomedical engineering from Shenzhen University, China, in 2017. She is currently with the Medical Instrument Lab, Shenzhen Academy of Metrology & Quality Inspection, Shenzhen, China. Her research interests include medical instruments and rehabilitation.

ZHEMIN ZHU received the M.S. degree in kinesiology and health science from Miami University, USA, in 2013. She was a Medical Interpreter with the Cincinnati Children's Hospital and a Coordinator with the Good Samaritan Hospital, OH, USA, before moving to Dublin, Ireland, in 2015. She is currently a Research Assistant with the Shenzhen Institute of Neuroscience, Shenzhen, China. Her research interests include the application of wearable technology in neurodegenerative diseases, motor learning and control, and the relationship between self-efficacy and the effects of exercise rehabilitation. She received the two-year's Grants from the Insight Centre for Data Analytics, Ireland.